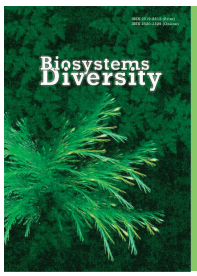

Biosystems Diversity

ISSN 2519-8513 (Print)
ISSN 2520-2529 (Online)
Biosyst. Divers., 2019,
27(2), 156–162
doi: 10.15421/011921

The temporal dynamics of readily available soil moisture for plants in the technosols of the Nikopol Manganese Ore Basin

O. M. Kunah*, Y. V. Zelenko**, M. P. Fedushko***, A. V. Babchenko****, V. O. Sirovatko*****, O. V. Zhukov*

*Oles Honchar Dnipro National University, Dnipro, Ukraine
**Dnipro National University of Railway Transport named after Academician V. Lazaryan, Dnipro, Ukraine
***Bogdan Khmelnitsky Melitopol State Pedagogical University, Melitopol, Ukraine
****Ukrainian State University of Chemical Technology, Dnipro, Ukraine
*****Dnipro Branch of State Institute of Ukrainian Soil Protection, Doslidne

Article info

Received 12.04.2019
Received in revised form 17.05.2019
Accepted 19.05.2019

Oles Honchar Dnipro National University, Gagarin av., 72, Dnipro, 49000, Ukraine. E-mail: kunah_olga@ukr.net Tel.: +38-098-858-23-79.

Dnipro National University of Railway Transport named after Academician V. Lazaryan, Lazaryan st., 2, Dnipro, 49010, Ukraine. E-mail: j.v.zelenko@gmail.com Tel.: +38-067-774-04-64.

Bogdan Khmelnitsky Melitopol State Pedagogical University, Hetmanska st., 20, Melitopol, 72318, Ukraine. E-mail: marinafedushko@gmail.com Tel.: +38-067-904-36-38.

Ukrainian State University of Chemical Technology, Gagarin av., 8, Dnipro, 49005, Ukraine. E-mail: lineanna83@gmail.com Tel.: +38-067-713-73-33.

Dnipro Branch of State Institute of Ukrainian Soil Protection, Naukova st., 65A, Doslidne, 52071, Ukraine. E-mail: rodgrunt_dp@i.ua Tel.: +38-097-259-67-96.

Kunah, O. M., Zelenko, Y. V., Fedushko, M. P., Babchenko, A. V., Sirovatko, V. O., & Zhukov, O. V. (2019). The temporal dynamics of readily available soil moisture for plants in the technosols of the Nikopol Manganese Ore Basin. Biosystems Diversity, 27(2), 156–162. doi:10.15421/011921

The restoration of a stable and productive ecosystem after drastic disturbances to the natural environment due to mining and open-cast mining may be achieved by means of reclamation. Investigation of the hydrological budget of technosols is important task in developing adequate approaches to reclamation. Sod lithogenic soils on red-brown clay, on grey-green clay were chosen as the objects of the investigation. The simulation of moisture content in Nikopol Manganese Ore Basin technosols was performed using the Penman-Monteith approach and evaluated the role of the dependence of soils' surface albedo on the humidity in the intensity of evapotranspiration. The research was conducted during 2013–2015 at the station for research on reclaimed land within the Nikopol Manganese Ore Basin (city Pokrov, Ukraine). The experimental area for the study of optimal modes of agricultural reclamation was created in 1968–1970. Precipitation in the investigated area was found to fall very unevenly in time. In 2013, the duration of the rainless period was 259 days, in 2014 – 264 days, in 2015 – 261 days. The maximum daily rainfall varies within 18–49 mm. There are significant interannual differences in the intensity of rainfall. The minimum total annual precipitation in 2014 was due to a decrease in atypical rainfall in late winter and early winter. The maximum annual rainfall in 2015 was caused by intense rainfall both in the spring and in mid-summer and late autumn. The average annual temperature was 11.1 ºC and the annual totals did not statistically significantly vary within the study period. The average wind speed and average atmospheric humidity are statistically significantly different from year to year. The technosols' colour properties and surface albedo varied depending on the moisture content. There is a linear relationship between the moisture content in the soil and albedo of the soil surface. The evaluation of readily available water content was carried out based on the Penman-Monteith model taking into account meteorological data, the water-physical properties of the technosols and the dependence of soil surface albedo on soil humidity. The distribution of this index for different technosols is characterized by a high level of similarity of shape due to the fact that the overall climate factors are crucial in shaping the dynamics of moisture. A complex mixture of normal distributions is the best model for representing the experimental data. The readily available water content distribution can best be represented as a mixture of two normal distributions. The relatively high moisture level is characterized for winter and spring periods. Water content in sod-lithogenic soils on red-brown clay over the period of research never reached the value of the permanent wilting point. In 2013, the period when the moisture content was less than the value of the permanent wilting point lasted 23 days, and in 2014 this period lasted 39 days. Thus, you can always expect the phenomenon of drought under typical climatic conditions for the technosols on grey-green clay. It was found that monitoring water supplies before the start of the growing season can provide valuable information necessary for the selection of crops for cultivation in the current year. The results indicate the urgency of measures to save the winter rainfall on the fields.

Keywords: reclamation; water regime; albedo; evapotranspiration; Penman-Monteith equation.

Introduction

Mining and open-cast mining cause drastic disturbances to the natural environment (Frouz, 2018). Reclamation can restore soil quality after mining over time, aiming at the restoration of a stable and productive ecosystem (Shrestha & Lal, 2011). The development of a water regime at post-mining sites can be divided into two parts: the development of soil, which stores water in the ecosystem, and the development of vegetation, which is an important consumer of water (Frouz, 2018). The land surface albedo, evapotranspiration, and surface roughness are the key factors of physical land-atmosphere interaction (Bonan, 2008). The hydrological budget is driven principally by precipitation and evapotranspiration (Rahgozar et al., 2012). These two climate elements largely determine the amount of moisture available for plant use or, in arid and semiarid regions, the magnitude of water deficiency (Toy, 1979). Differences in transpiration water rate of soil may be deduced by the ground biomass and vegetation cover which are different in soils with different organic layer thickness (Scherbina et al., 2014; Tromp-van Meerveld & McDonnell, 2006). Evapotranspiration is the key element of land water balance structure (Hlaváčiková & Novák, 2013). Variation in transpiration water rate considerably effects the spatial distribution of soil moisture (Detto et al., 2006). In semiarid regions, evapotranspiration is the leading loss term of the root zone water budget (Reynolds et al., 2000; Williams & Albertson, 2004).

Various modelling approaches have been used for estimation of evapotranspiration at regional scales (Ray & Dadhwal, 2001; Consoli et al., 2006; Tasumi & Allen, 2007). There are direct and indirect methods for evapotranspiration estimation (Chanasyk et al., 2006). Indirect

methods include those based on the concept of actual evapotranspiration versus potential evapotranspiration and utilize meteorological data (Sharma, 1985). At the field scale, a model for determining wheat basal crop coefficients from observations of the normalized difference vegetation index (NDVI) were developed (Hunsaker et al., 2005). The daily evapotranspiration was computed from instantaneous latent heat flux estimates derived from digital airborne multispectral remote sensing imagery (Chavez et al., 2008). The FAO Penman-Monteith reference evapotranspiration equation is one of the basic tools to calculate evapotranspiration from meteorological data (Penman, 1948; Allen et al., 1998). The Penman-Monteith equation has been revealed to be reliable in a wide range of environments (Hess, 1996). Its computation requires weather data on maximum and minimum temperature, solar radiation, relative humidity and wind speed at 2 m height. This approach was tested and validated (Pereira et al., 2003; Popova et al., 2006; Jabloun & Sahli, 2008). The first step of actual evapotranspiration estimation includes the calculating potential evapotranspiration from meteorological data using equations based on the aerodynamic theory and energy balance (Penman, 1948; Monteith, 1965). The potential evapotranspiration is then used to estimate actual evapotranspiration after application the soil water reduction factor, which is based on available or extractable soil water (Slabbers, 1980). The reference crop evapotranspiration is the evapotranspiration from a crop with specific characteristics. FAO-56 method sets the specific characteristics of a reference crop with certain height (0.12 m), surface resistance (70 s m^{-1}) and albedo (0.23) and then determines the reference evapotranspiration using the Penman-Monteith equation (Allen et al., 1998). The albedo was shown to be able to considerably effect the evapotranspiration rate (Seginer, 1969). Albedo is a leading factor in terms of climate impact (Zeng & Yoon, 2009). The effect of albedo on potential evapotranspiration varies with the season. Albedo has its greatest influence in the summer months (Jackson, 1967). Albedo is dependent on the soil cover colour (Post et al., 2000). Soil colour was detected to change after reclamation (Singh et al., 2015).

Artificial soils formed in the process of reclamation are classified as technosols. These manufactured soils have specific physical and chemical characteristics along with potential toxicity problems (Leguédois et al., 2016; Maltsev et al., 2017). Technosols were shown to perform ecosystem services such as water regulation (Huot et al., 2015). Research on physical properties of soil plays a significant role for the evaluation of reclamation success (Dexter, 2004). Soil thickness, texture (Brygadyrenko, 2015a, 2015b, 2016a, 2016b), bulk density, porosity, pH (Klimkina et al., 2018; Shcherbyna et al., 2017), soil mass water content, soil mechanical impedance (Zhukov et al., 2015), soil gravel content, and soil electrical conductivity (Zhukov et al., 2016) are the important indicators for assessing the physical properties of reconstructed soils (Arshad & Martin, 2002). Reclamation enhances soil quality by improving physical and chemical properties, which helps in restoration of mine soils (Shrestha & Lal, 2008). Considerable changes of the soil bulk density, soil porosity, and soil mass water content were revealed to have taken place after a long time of vegetation restoration (Cao et al., 2015). After the rehabilitation period, the content of water available for plants was found to be favourable in reclaimed soils but less beneficial conditions of the soil were associated with air and water permeability (Kofodziej et al., 2016). Saturated hydraulic conductivity was found to increase in agricultural reclamation as a result of tillage and alfalfa cultivation (Krümmelbein et al., 2010; Krümmelbein & Raab, 2012). Water holding capacity was near to that of the reference sites after 25 years of reclamation (Singh et al., 2015).

The aim of the study is to perform a simulation of moisture content in technosols of the Nikopol Manganese Ore Basin using the Penman-Monteith approach and evaluate the role of the dependence of the soils' surface albedo on the humidity in the intensity of evapotranspiration.

Materials and methods

The research was conducted during the years 2013–2015 at the station for research on reclaimed land within the Nikopol Manganese Ore Basin (city Pokrov, Ukraine). The experimental area for the study of optimal modes of agricultural reclamation was created during the years 1968–1970. The sod lithogenic soils on red-brown clay, on grey-green clay were chosen as the objects of the investigation. Technosols are characterized by the following water-physical properties (the amount of moisture in the soil layer thickness of 1 m). Sod-lithogenic soils on red-brown clay loams: field capacity – 317.41 mm, available soil moisture – 212.57 mm, maximum hygroscopic moisture – 77.90 mm, permanent wilting point – 104.83. Sod-lithogenic soils on the grey-green clay: field capacity – 419.32 mm, available soil moisture – 197.30 mm, maximum hygroscopic moisture – 165.12 mm, permanent wilting point – 222.02 mm (Zhukov et al., 2017). The presented hydrological constants were used in further calculations.

The evapotranspiration from the soil surface was calculated by means of the Penman-Monteith equation (Monteith, 1965):

$$E_{ref} = \frac{0.408\Delta(R_n - G_0) + \gamma \frac{900}{T_d + 273} u_2 (e_d - e_a)}{\Delta + \gamma(1 + 0.34u_2)}, \quad (1)$$

where E_{ref} is reference evapotranspiration rate (mm d^{-1}), R_n – net radiation flux (MJ $m^{-2}d^{-1}$), G_0 – sensible heat flux into the soil (MJ $m^{-2}d^{-1}$), T_d – mean air temperature (°C), u_2 – wind speed (m s^{-1}) at 2 m above the ground, e_d is saturated vapour pressure at temperature T_d (ºC):

$$e_d = 0.611 \exp\left(\frac{17.27T_d}{T_d + 237.3}\right), \quad (2)$$

Δ is the slope of the vapour pressure curve, γ is the psychrometric constant (kPa $°C^{-1}$), e_d–e_a – is saturated vapour pressure deficit.

Actual evapotranspiration may be calculated as follows:

$$E_{act} = K_s E_{ref}, \quad (3)$$

where K_s – water stress factor.

Root zone moisture depletion is evaluated as the difference between soil water content at field capacity (pF = 2.3) and actual soil water content. The K_s value which is a water stress factor equals 1.0 as long as soil water content is higher than readily available water (a fraction of the total available water). If soil water content is lower than readily available water (RAW), K_s decreases linearly from one to zero according to total available soil water consumed.

The following equation for calculating the daily net radiation was applied (Allen et al., 1994a, b):

$$R_n = (1 - \alpha)R_{si} - \left[a_c\left(\frac{R_{si}}{R_{so}}\right) + b_c\right](a_1 + b_1 e_d^{0.5})\sigma\left(\frac{T_m^4 + T_n^4}{2}\right), \quad (4)$$

where σ is the Stefan-Boltzmann constant ($\sigma = 4.903 \times 10^{-9}$ MJ $K^{-4}m^{-2}$), T_m and T_n represent the maximum and minimum air temperatures (ºC) in one day, respectively, a_c and b_c are the cloud factors, equal to 1.35 and –0.35, respectively, a_1 and b_1 are the emissivity factors, equal to 0.35 and –0.14, respectively (Evett et al., 2011), α is the soil surface albedo depending on the soil water content, colour and texture as well as the organic matter content and surface roughness. R_{si}/R_{so} is the relative short-wave radiation, which is used to express the cloudiness of the atmosphere. When the sky is cloudier, its value is smaller. It varies in the range from 0.33 (dense cloud cover) to 1 (clear sky) (Allen et al., 1998).

The solar radiation in case of clear sky, R_{so}, is expressed as:

$$R_{so} = (0.75 + 0.00002EL_{msl})R_{sa}, \quad (5)$$

where EL_{msl} is the elevation (m) above the mean sea level; and R_{sa} is the extraterrestrial solar radiation, which can be calculated by (Evett et al., 2011):

$$R_{sa} = \left[\frac{24(60)}{\pi}\right] G_{sc} d_r (\cos\theta\cos\delta\sin\omega_s + \omega_s\sin\theta\sin\delta), \quad (6)$$

where

$$d_r = 1 + 0.33\cos\left(\frac{2\pi J}{365}\right), \quad (7)$$

$$\omega_s = \cos^{-1}(-\tan\theta\tan\delta), \quad (8)$$

the term 24(60)/π is the inverse angle of rotation in daily; G_{sc} is the solar constant (–0.08202 MJ $m^{-2}min^{-1}$); dr is the relative distance between the Earth and the sun (m); J is the day of year; ωs is the sunset time angle (rad), the angle from solar noon to sunset; θ is the latitude; and δ is the solar declination.

The relationship between the 0.3–2.8 mm soil albedo and the Munsell colour value component has the form (Post et al., 2000):

$$Y = -0.11 + 0.07X, \quad (9)$$

where Y – albedo, X – Munsell colour value component.

The soil samples were dried and artificially adjusted to ten levels of humidity in the range of the maximum hygroscopic moisture to the field capacity that are inherent for each technosol type. The digital image was made for each level of humidification in which colour characteristics in RGB-format were quantitatively measured using ImageJ software (Schneider et al., 2012). Colour specification in RGB-format was converted to the Munsell colour system using rgb2munsell library aqp (Beaudette et al., 2013) for Project R (R Core Team, 2018). Based on the equation (9) for colour, albedo properties were evaluated for each respective technosol gradation, allowing regression to find the relationship between soil moisture and albedo.

The soil water balance is performed in ISAREG (Teixeira & Pereira, 1992) with a daily time step as:

$$SW_i = SW_{i-1} + P_i + I_i + G_i - E_i - D_i, \quad (10)$$

where SW_i and SW_{i-1} are respectively the soil water storage (mm) in the soil layer zone at the end of day i and of the previous day, i–1; P_i is the precipitation; I_i is the net irrigation depth; G_i is the capillary rise; E_i is the actual evapotranspiration, and D_i is the deep percolation out of the root zone, all referring to day i. All units but for SW are in mm d^{-1}. I_i, G_i, and D_i were neglected in this application.

Readily available water was found as:

$$RAW_i = SW_i - PWP, \quad (11)$$

where RAW – readily available water (mm), SW_i is the soil water storage (mm), PWP – permanent wilting point (mm).

Statistical calculation were made using software Statistica (version 8, StatSoft Inc., USA).

Results

Precipitation falls very unevenly in time on the investigated area. In 2013, the duration of rainless period was 259 days in 2014 – 264 days, in 2015 – 261 days. The maximum daily rainfall varied within 18–49 mm (Table 1).

Table 1
Descriptive statistics of the daily meteorological characteristics based on observations at meteorological stations Nikopol (2013–2015)

Parameters	x ± SE	Median	Minimum	Maximum	CV, %
2013, N = 365					
Precipitation, mm	0.95 ± 0.15	0.00	0.00	20.00	302.06
Wind speed, m/s	2.39 ± 0.06	2.25	0.25	7.00	47.35
Temperature, ºC	11.33 ± 0.50	10.96	–9.57	28.21	83.75
T_{min}, ºC	7.49 ± 0.43	6.70	–12.40	22.00	109.66
T_{max}, ºC	15.10 ± 0.57	14.40	–6.40	34.30	72.42
Atmospheric humidity, %	73.37 ± 0.78	73.75	38.13	99.88	20.43
Atmospheric pressure, gPa	1014.85 ± 0.39	1014.00	992.21	1036.43	0.74
2014, N = 365					
Precipitation, mm	0.90 ± 0.15	0.00	0.00	18.00	308.39
Wind speed, m/s	2.28 ± 0.07	2.00	0.00	8.86	59.77
Temperature, ºC	10.89 ± 0.56	10.93	–17.72	30.28	97.96
T_{min}, ºC	6.47 ± 0.49	5.80	–21.30	22.20	146.02
T_{max}, ºC	15.17 ± 0.62	16.00	–15.10	37.80	78.51
Atmospheric humidity, %	69.12 ± 0.91	69.57	27.75	100.00	25.08
Atmospheric pressure, gPa	1014.67 ± 0.40	1014.13	992.55	1047.33	0.75
2015, N = 365					
Precipitation, mm	1.39 ± 0.23	0.00	0.00	49.00	320.11
Wind speed, m/s	2.00 ± 0.08	1.50	0.00	8.50	73.90
Temperature, ºC	11.21 ± 0.51	10.23	–20.84	30.09	87.37
T_{min}, ºC	6.43 ± 0.45	5.20	–23.40	23.50	134.06
T_{max}, ºC	15.88 ± 0.58	14.70	–17.20	36.70	70.28
Atmospheric humidity, %	69.59 ± 0.83	67.75	35.43	99.25	22.78
Atmospheric pressure, gPa	1009.26 ± 0.43	1008.90	983.16	1034.64	0.82

The highest amount of precipitation fell in the year 2015 (506.8 mm), and the lowest – in 2014 (328.9 mm). In 2013 precipitation was 345.6 mm. The intensity of the rainfall varies throughout the year. The highest rainfall usually occurs in June and the lowest – in August (Table. 2). There are significant interannual differences in the intensity of rainfall. Minimum total annual precipitation in 2014 was due to a decrease in atypical rainfall in late winter and early winter. Maximum annual rainfall in 2015 was caused by intense rainfall both in the spring and in mid-summer and late autumn. The average annual temperature was 11.14 ± 0.30 ºC and was not statistically significant different between years during the study period (F = 0.19, P = 0.82). The temperature range was from –23.4 to + 37.8 ºC during the study period. Minimum temperatures occur in January or February, and the maximum temperatures – in July or August. The largest temperature fluctuations occur in the winter or spring. The autumn period is usually marked by the sharp fall of temperatures.

Table 2
The distribution of monthly precipitation during 2013–2015 (mm)

Month	Year		
	2013	2014	2015
January	43.60	21.40	18.70
February	15.00	5.20	44.60
March	57.10	7.40	74.60
April	7.30	36.40	62.80
May	19.20	47.20	50.30
June	73.00	64.30	84.60
July	21.00	10.20	83.10
August	3.20	16.80	19.10
September	45.70	31.00	2.00
October	51.10	26.70	7.30
November	5.30	15.60	58.00
December	4.10	46.70	1.70
Total	345.60	328.90	506.80

The winds blew predominantly from the east and north direction (in 2013), from the east and northeast direction (in 2014) or from the north and northeast direction (in 2015). The average wind speed is statistically significantly different from year to year (F = 8.72, P < 0.001). The highest wind speed was observed in 2013, and the lowest – in the 2015 (Table 3). The wind speed local maximum was observed in March and autumn. The wind speed local minimum occurs in late summer. From the patterns indicated there are significant deviations from year to year. Thus, in 2014 the maximum wind speed was observed in January. In 2013 there was a minimum wind speed in June, after which there was a monotonic trend of increasing wind speed.

Table 3
The distribution of monthly average wind speed during 2013–2015 (m/s)

Month	Year		
	2013	2014	2015
January	2.31	3.59	2.60
February	2.89	2.45	2.73
March	3.17	3.50	3.36
April	2.38	2.37	2.62
May	1.94	2.00	1.84
June	1.83	2.37	1.38
July	1.90	2.42	1.33
August	2.12	1.30	1.32
September	2.34	2.09	1.81
October	2.29	1.78	1.16
November	2.72	1.65	2.03
December	2.90	1.84	1.80
Average	2.40	2.28	2.00

The average atmospheric humidity statistically significantly varied from year to year (F = 7.67, P < 0.001). The highest humidity was found in 2013, differences in the level of humidity in 2014 and 2015 were not significant (Table 4). From the beginning of the year, there was a monotonic decrease in humidity until August, when there was a minimum of this indicator. The growth of humidity was detected in autumn, sometimes very quickly to the maximum values in winter. The atmospheric humidity is depended on the other climatic indicators.

The mean atmospheric pressure statistically significantly varied from year to year (F = 60.22, P < 0.001). The lowest atmospheric pressure was observed in 2015 (Table 5). The difference between 2013 and 2014 was not statistically significant. The highest value of the atmospheric pressure is typical of early winter, and then in spring pressure was quite sharply reduced. In May, there was usually minimum of the atmospheric pressure, followed by a gradual increase, which took a sharp character from the middle of autumn.

Table 4
The distribution of monthly average atmospheric humidity during 2013–2015 (%)

Month	Year		
	2013	2014	2015
January	91.51	78.60	87.52
February	82.02	84.23	78.93
March	75.45	61.91	71.16
April	65.29	65.97	66.91
May	62.99	68.94	63.79
June	62.45	63.28	68.15
July	61.53	53.96	64.43
August	55.21	51.99	49.93
September	74.17	56.23	56.52
October	84.81	72.64	62.21
November	82.19	83.14	83.34
December	83.43	89.91	83.08
Average	73.42	69.23	69.66

Table 5
The distribution of monthly average atmospheric pressure during 2013–2015 (gPa)

Month	Year		
	2013	2014	2015
January	1012.2	1022.8	1007.3
February	1016.3	1022.3	1007.9
March	1009.9	1015.2	1010.9
April	1015.6	1015.4	1002.5
May	1011.1	1013.5	1003.2
June	1010.0	1012.1	1006.4
July	1012.1	1011.9	1006.5
August	1014.1	1006.3	1010.0
September	1011.7	1010.1	1010.5
October	1022.0	1015.9	1016.5
November	1019.2	1017.9	1008.8
December	1024.4	1013.0	1020.5
Average	1014.8	1014.7	1009.3

The technosols colour properties and its surface albedo vary depending on the moisture content. The colour of the surface of the sod-lithogenic soil on the red-brown clay varies from yellow-red (5YR 4/8) in wet condition to red (10R 9/9) in the dry condition (Table 6). Albedo depended on the humidity varies in the range 0.17–0.52.

Table 6
The variability of the albedo and surface colour characteristics of the technosols depending on water content

Water content, mm in 1 meter soil layer	Munsell colour properties			Albedo*
	Hue	Value	Chroma	
Sod-lithogenic soil on the red-brown clay				
78.0	10R	9.0	9	0.52
105.6	2.5YR	8.0	8	0.45
133.2	2.5YR	7.5	10	0.42
160.7	10R	7.0	9	0.38
188.3	10R	6.5	12	0.35
206.7	2.5YR	6.0	11	0.31
234.3	2.5YR	5.5	10	0.28
261.8	2.5YR	5.0	9	0.24
289.4	2.5YR	4.8	9	0.23
317.0	5YR	4.0	8	0.17
Sod-lithogenic soil on the grey-green clay				
162.0	5G	9.0	1	0.52
191.7	5G	8.5	1	0.49
221.4	5G	7.7	5	0.43
251.1	4G	7.2	4	0.39
280.8	4G	6.6	4	0.35
300.6	4G	6.4	4	0.34
330.2	3G	6.0	3	0.31
359.9	3G	5.8	3	0.30
389.6	2.5G	5.4	3	0.27
419.3	2.5G	5.0	3	0.24

Note: * – estimation on the basis of the equation Y = –0.11 + 0.07 X, where Y – albedo, X – Munsell colour value component (Post et al., 2000).

The colour of the surface of the sod-lithogenic soil on the grey-green clay varies from very dark greyish green (5YR 4/8) in wet condition to greyish green (10R 9/9) in the dry condition. Albedo of this soil dependent on the humidity varies in the range 0.24–0.52. There is a linear relationship between the moisture content in the soil and albedo of the soil surface. Albedo changes along with the humidity are most significant in the sod-lithogenic soils on red-brown clay. This is confirmed by the greatest regression coefficient.

The evaluation of readily available water content was carried out based on the Penman-Monteith model taking into account meteorological data, the technosols' water-physical properties and the dependence of soil surface albedo on soil humidity. The distribution of this index for different technosols was characterized by a high level of similarity of shape due to the fact that the overall climate factors are crucial in shaping the dynamics of moisture. The distributions are asymmetric, which is also confirmed by the skewness coefficients that are statistically significantly different from zero (Table 7).

Table 7
Descriptive statistics of the readily available water content

Soil	x ± SE, mm	Minimum, mm	Maximum, mm	Skewness ± SE	Kurtosis ± SE
2013					
RB	118.95 ± 3.41	17.45	213.34	0.29 ± 0.13	–1.31 ± 0.25
GG	99.30 ± 3.57	–6.42	197.65	0.28 ± 0.13	–1.34 ± 0.25
2014					
RB	65.03 ± 1.38	6.27	108.57	–0.60 ± 0.13	–0.82 ± 0.25
GG	40.33 ± 1.43	–20.20	82.21	–0.58 ± 0.13	–0.87 ± 0.25
2015					
RB	124.69 ± 2.54	41.25	213.34	–0.23 ± 0.13	–1.20 ± 0.25
GG	105.14 ± 2.59	20.90	197.65	–0.19 ± 0.13	–1.21 ± 0.25
Total					
RB	102.89 ± 1.70	6.27	213.34	0.53 ± 0.07	–0.73 ± 0.15
GG	81.59 ± 1.78	–20.20	197.65	0.54 ± 0.07	–0.73 ± 0.15

Notes: RB – on the red-brown clay; GG – on the grey-green clay.

A complex mixture of normal distributions is the best model to represent the experimental data. The readily available water content distribution of sod-lithogenic soils on red-brown clay can best be represented as a mixture of two normal distributions (Kolmogorov-Smirnov statistic d = 0.04, P = 0.18). The first mixture component holds 0.73 of the total variation (mean = 73.5, σ = 30.1), the second – 0.27 of the total variation (mean = 182.4, σ = 24.1). A relatively high moisture level is characterized for winter and spring periods (Fig. 1). Typically, heavy rainfall in early summer recharged soil water content. The exception was in 2014, when summer precipitations were minor and did not affect significantly the level of moisture reserves. However, water content in sod-lithogenic soils on red-brown clay over the period of research never reached the value of the permanent wilting point.

A mixture of three normal distributions is the best model for the distribution of readily available water in the sod-lithogenic soils on the grey-green clay (Kolmogorov-Smirnov statistics d = 0.045, P = 0.15). The first mixture component holds the 0.72 of the total variation (mean = 50.1, σ = 30.8), the second – 0.28 of the total variations (mean = 163.4, σ = 26.7). The relatively high levels of water reserves are characteristic for winter and spring periods. These tend to recharge as a result of the high rainfall in early summer. The recharge was sufficient in the year 2015, whereas in 2013 and in 2014 there was a drought in the summer. In 2013 the period when the moisture content was less than the value of the permanent wilting point lasted 23 days, and in 2014 this period lasted 39 days. Thus, you can always expect the phenomenon of drought under typical climatic conditions for the technosols on grey-green clay.

Discussion

The dynamics of the soil moisture content can be modeled by the balance of precipitation and evapotranspiration intensity in conditions of the non-washing water regime of the soil. The routine meteorological data can be used to simulate the balance of water and evapotranspiration

(Allen et al., 1998). Besides climatic regimes, the water-physical properties of the particular soil type play a key role in water dynamics. Albedo of the soil surface is particularly important. In this regard the technosols as young soil-like bodies are characterized by considerable colour diversity. Albedo essentially depends on the colour of the soil surface (Post et al., 2000). The colour of the upper soil layers is dependent on organic matter content which gives it colours from grey to black. The technosols' organic matter content is low in the early stages of development, so technosols encompass a diverse range of colours. The pedozem is most similar to natural analogues in structure and colour of the surface and is characterized by the lowest albedo. The technosols that formed on the grey-green clay have the highest albedo value. It should be noted albedo is dependent on the moisture content: wet soils are characterized by a lower albedo. Also, higher organic matter content decreases albedo. Thus, the evapotranspiration rate decreases due to increased albedo with the decrease of water content in soil.

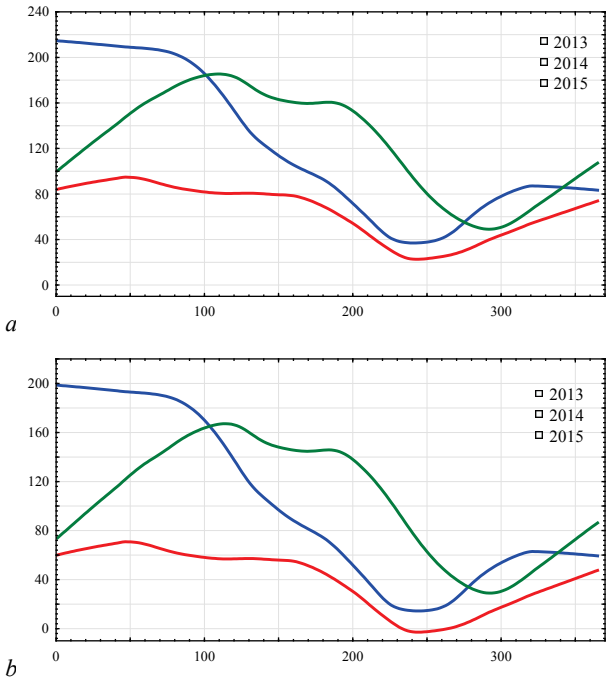

Fig. 1. The temporal dynamics of readily available soil moisture in the sod-lithogenic soils on red-brown clay (*a*) and on the sod-lithogenic soils on grey-green clay (*b*): the horizontal axis is the order of the days of the year, the vertical axis is readily available soil moisture (mm); 2013, 2013, 2015 – the soil moisture series of each year studied; The lines indicate a lowess-approximation

The general trend of the readily available soil moisture variation is very similar for all studied technosols. The differences relate to quantitative characteristics, which are caused by the water-physical properties. The field capacity is attributable mainly to the soil aggregation structure (Frouz, 2018). The investigated soils are clay or loam, which have a high ability to aggregate formation. The low humus content makes aggregates water unstable (Frouz & Kuráž, 2014). Organic matter can improve bulk density of the technosols, its aeration and water retention/infiltration (Sanborn et al., 2004), aggregation and structure (Larney & Angers, 2012). In loess used for reclamation $CaCO_3$ as cementing agent dominates soil aggregation (Pihlap et al., 2019).

Also salinity processes in technosols do not contribute to the formation of water stable aggregate structure (Klimkina et al., 2018). However, all technosols studied have the high rates of field capacity, which determines the range of available soil moisture. The permanent wilting point is a function of soil granulometric composition (Bradshaw, 1997) and, in conditions of salinity, this parameter is affected on the content of soluble salts (Shrestha & Lal, 2011). Clay and loamy particle size generates high values of permanent wilting point.

This study examined the year with relatively high precipitation (2015), during which rain fell almost 50% more than in the rest of the studied years. The years 2013 and 2014 are characterized by similar precipitation values. But the peculiarities of the readily available soil moisture dynamics in the years are significantly different, due to the different patterns of rainfall during the year. In 2015 the duration of summer, when precipitation falls, was significantly extended, resulting generated optimal conditions for plants growth. In the 2013 summer peak rainfall was not long, but it was enough to compensate for the intense summer evaporation. The rainfall deficit in the winter of 2013–2014 does not made it possible to create the necessary supply of moisture before the growing season. Almost until the middle of summer moisture level in the soil was constant, but in late summer it fell sharply. This is even despite the fact that during April–June precipitation in 2014 was even slightly higher than in 2013.

The specifics of albedo dynamics depending on moisture content and technosols' water-physical properties create the preconditions for the formation of water regime stability. The stability of the water regime allows for sufficient moisture available for plants within a significant range of vegetation. Even crops with a long vegetation period most sensitive to water shortages can finish their life cycle on technosols under conditions of heavy rainfall at the beginning of the summer. But unfortunately, the considerable supplies of moisture in spring do not guarantee this. Initial indicators of moisture content in 2013 and 2015 were almost the same, but no significant rainfall in early summer 2013 led the dynamics of moisture content to the level of 2014, when the starting conditions were much worse.

A common feature of global warming is the increase in precipitation and change in its time patterns. As shown by the results of our research, reduction in the norms of precipitation in the winter period significantly affects the mode of moisture during the growing season. On the other hand, favourable moisture reserves in the spring do not guarantee an optimal water regime during the growing season, which is possible only in conditions of high levels of rainfall in early summer, but the latter is a random event and cannot be accurately estimated. With this in mind, the following practical recommendations can be made. First, monitoring of water supplies before the start of the growing season can provide valuable information necessary for the selection of crops for cultivation in the current year. Secondly, the results indicate the urgency of measures to save the winter rainfall on the fields. Thirdly, it is recommended to use mulch to conserve moisture, including by increasing the albedo of the surface soil.

Conclusion

Obviously, the meteorological conditions are most important factors that determine the dynamics of moisture content in all soil, including artificial. The water regime features of technozems depend on their water-physical properties and characteristics of the soil contact surface with the environment. Vegetation, colour and character of the soil surface greatly affect the intensity of energy and material exchange with the soil environment. The technozems are young soils, which have a large variability in surface colour. This feature leads to a significant variation of surface albedo of technosols. The relationship between albedo and moisture creates the preconditions for the formation of the negative feedback mechanism of communication between the humidity and the evapotranspiration intensity. Reducing the water content in the soil leads to reduction of evaporation due to increased albedo. It should be noted that over the soil forming process the colour differences between technosols will decrease due to the accumulation of organic matter that provides soils, black or grey. But the accumulation of organic matter improves the technosols' water-physical properties enabling better use of the climate potential.

References

Allen, R. G., Pereira, L. S., Raes, D., & Smith, M. (1998). Crop evapotranspiration: Guidelines for computing crop water requirements. Irrigation and Drainage Paper 56. Rome, Italy: Food and Agriculture Organization of the United Nations. Pp. 1–15.

Allen, R. G., Smith, M., Perrier, A., & Pereira, L. S. (1994a). An update for the definition of reference evapotranspiration. ICID Bulletin, 43(2), 1–34.

Allen, R. G., Smith, M., Perrier, A., & Pereira, L. S. (1994b). An update for the definition of reference evapotranspiration. ICID Bulletin, 43(2), 35–92.
An, N., Hemmati, S., & Cui, Y.-J. (2017). Assessment of the methods for determining net radiation at different time-scales of meteorological variables. Journal of Rock Mechanics and Geotechnical Engineering, 9, 239–246.
Arshad, M. A., & Martin, S. (2002). Identifying critical limits for soil quality indicators in agro-ecosystems. Agriculture, Ecosystems and Environment, 88(2), 153–160.
Beaudette, D. E., Roudier, P., & O'Geen, A. T. (2013). Algorithms for quantitative pedology: A toolkit for soil scientists. Computers and Geosciences, 52, 258–268.
Bonan, G. B. (2008). Forests and climate change: Forcings, feedbacks, and the climate benefits of forests. Science, 320(5882), 1444–1449.
Bradshaw, A. (1997). Restoration of mined lands – Using natural processes. Ecological Engineering, 8(4), 255–269.
Brygadyrenko, V. V. (2015a). Community structure of litter invertebrates of forest belt ecosystems in the Ukrainian steppe zone. International Journal of Environmental Research, 9(4), 1183–1192.
Brygadyrenko, V. V. (2015b). Evaluation of the ecological niche of some abundant species of the subfamily Platyninae (Coleoptera, Carabidae) against the background of eight ecological factors. Folia Oecologica, 42(2), 75–88.
Brygadyrenko, V. V. (2016a). Evaluation of ecological niches of abundant species of Poecilus and Pterostichus (Coleoptera: Carabidae) in forests of the steppe zone of Ukraine. Entomologica Fennica, 27(2), 81–100.
Brygadyrenko, V. V. (2016b). Influence of litter thickness on the structure of litter macrofauna of deciduous forests of Ukraine's steppe zone. Visnyk of Dnipropetrovsk University. Biology, Ecology, 24(1), 240–248.
Cao, Y. G., Wang, J. M., Bai, Z. K., Zhou, W., Zhao, Z. Q., Ding, X., & Li, Y. (2015). Differentiation and mechanisms on physical properties of reconstructed soils on open-cast mine dump of loess area. Environmental Earth Sciences, 74(8), 6367–6380.
Chanasyk, D. S., Mapfumo, E., & Chaikowsky, C. L. A. (2006). Estimating actual evapotranspiration using water budget and soil water reduction methods. Canadian Journal of Soil Science, 86(4), 757–766.
Chavez, J., Neale, C. M. U., Prueger, J. H., & Kustas, W. P. (2008). Daily evapotranspiration estimates from extrapolating instantaneous airborne remote sensing ET values. Irrigation Science, 27(1), 67–81.
Consoli, S., D'Urso, G., & Toscano, A. (2006). Remote sensing to estimate ET-fluxes and the performance of an irrigation district in southern Italy. Agricultural Water Management, 81, 295–314.
Detto, M., Montaldo, N., Albertson, J. D., Mancini, M., & Katul, G. (2006). Soil moisture and vegetation controls on evapotranspiration in a heterogeneous Mediterranean ecosystem on Sardinia, Italy. Water Resources Research, 42(8), 1–16.
Dexter, A. R. (2004). Soil physical quality. Part I. Theory, effects of soil texture, density, and organic matter, and effects on root growth. Geoderma, 120, 201–214.
Dexter, A. R., & Richard, G. (2009). The saturated hydraulic conductivity of soils with n-modal pore size distributions. Geoderma, 154, 76–85.
Evett, S. R., Prueger, J. H., & Tolk, J. A. (2011). Water and energy balances in the soil-plantatmosphere continuum. In: Huang, P. M., Li, Y., & Sumner, M. E. (Eds.). Handbook of soil sciences: Properties and processes. 2nd ed. CRC Press, Boca Raton.
Frouz, J. (2018). Changes of water budget during ecosystem development in post-mining sites at various spatiotemporal scales: The need for controlled systems. Hydrology of Artificial and Controlled Experiments, 95–106.
Frouz, J., & Kuráž, V. (2014). Soil fauna and soil physical properties. In: Frouz, J. (Ed.). Soil biota and ecosystem development in post mining sites. CRC Press, Boca Raton.
Hess, T. M. (1996). Evapotranspiration estimates for water balance scheduling in the UK. Irrigation News, 25, 31–36.
Hlaváčiková, H., & Novák, V. (2013). Comparison of daily potential evapotranspiration calculated by two procedures based on Penman-Monteith type equation. Journal of Hydrology and Hydromechanics, 61(2), 173–176.
Hunsaker, D. J., Pinter, P. J., & Kimball, B. A. (2005). Wheat basal crop coefficients determined by normalized difference vegetation index. Irrigation Science, 24(1), 1–14.
Huot, H., Séré, G., Charbonnier, P., Simonnot, M. O., & Morel, J. L. (2015). Lysimeter monitoring as assessment of the potential for revegetation to manage former iron industry settling ponds. Science of the Total Environment, 526, 29–40.
Jabloun, M., & Sahli, A. (2008). Evaluation of FAO-56 methodology for estimating reference evapotranspiration using limited climatic data: Application to Tunisia. Agricultural Water Management, 95(6), 707–715.
Jackson, R. J. (1967). The effect of slope, aspect and albedo on potential evapotranspiration from hillslopes and catchments. Journal of Hydrology (New Zealand), 6(2), 60–69.
Klimkina, I., Kharytonov, M., & Zhukov, O. (2018). Trend analysis of water-soluble salts vertical migration in technogenic edaphotops of reclaimed mine dumps in Western Donbass (Ukraine). Journal of Environmental Research, Engineering and Management, 74(2), 82–93.
Kofodziej, B., Bryk, M., Sfowińska-Jurkiewicz, A., Otremba, K., & Gilewska, M. (2016). Soil physical properties of agriculturally reclaimed area after lignite mine: A case study from central Poland. Soil and Tillage Research, 163, 54–63.
Krümmelbein, J., & Raab, T. (2012). Development of soil physical parameters in agricultural reclamation after brown coal mining within the first four years. Soil and Tillage Research, 125, 109–155.
Krümmelbein, J., Horn, R., Raab, T., Bens, O., & Hüttl, R. (2010). Soil physical parameters of a recently established agricultural recultivation site after brown coal mining in Eastern Germany. Soil and Tillage Research, 111, 19–25.
Larney, F. J., & Angers, D. A. (2012). The role of organic amendments in soil reclamation: A review. Canadian Journal of Soil Science, 92(1), 19–38.
Leguédois, S., Séré, G., Auclerc, A., Cortet, J., Huot, H., Ouvrard, S., Watteau, F., Schwartz, C., & Morel, J. L. (2016). Modelling pedogenesis of technosols. Geoderma, 262, 199–212.
Maltsev, Y. I., Didovich, S. V., & Maltseva, I. A. (2017). Seasonal changes in the communities of microorganisms and algae in the litters of tree plantations in the steppe zone. Eurasian Soil Science, 50(8), 935–942.
Maslikova, K. P., Ladska, I. V., & Zhukov, O. V. (2016). Permeability of soils in artificially created models with different stratigraphy. Biological Bulletin of Bogdan Chmelnitskiy Melitopol State Pedagogical University, 6(3), 234–247.
Monteith, J. L. (1965). Evaporation and the environment. In: The state and movement of water in living organisms. 19th Symposium of the Society for Experimental Biology. Cambridge University Press, London. Pp. 205–234.
Penman, H. L. (1948). Natural evaporation from open water, bare soil, and grass. Proceedings of the Royal Society of London. Series A, Mathematical and Physical Sciences, 193(1032), 120–145.
Pereira, L. S., Cai, L. G., & Hann, M. J. (2003). Farm water and soil management for improved water use in the North China Plain. Irrigation and Drainage, 52(4), 299–317.
Pihlap, E., Vuko, M., Lucas, M., Steffens, M., Schloter, M., Vetterlein, D., Endenich, M., & Kögel-Knabner, I. (2019). Initial soil formation in an agriculturally reclaimed open-cast mining area – the role of management and loess parent material. Soil and Tillage Research, 191, 224–237.
Popova, Z., Eneva, S., & Pereira, L. S. (2006). Model validation, crop coefficients and yield response factors for maize irrigation scheduling based on long-term experiments. Biosystems Engineering, 95(1), 139–149.
Post, D. F., Fimbres, A., Matthias, A. D., Sano, E. E., Accioly, L., Batchily, A. K., & Ferreira, L. G. (2000). Predicting soil albedo from soil color and spectral reflectance data. Soil Science Society of America Journal, 64, 1027–1034.
R Core Team (2017). R: A language and environment for statistical computing. R Foundation for Statistical Computing, Vienna.
Rahgozar, M., Shah, N., & Ross, M. (2012). Estimation of evapotranspiration and water budget components using concurrent soil moisture and water table monitoring. ISRN Soil Science, 2012, 726806.
Ray, S. S., & Dadhwal, V. K. (2001). Estimation of crop evapotranspiration of irrigation command area using remote sensing and GIS. Agricultural Water Management, 49(3), 239–249.
Reynolds, J., Kemp, P., & Tenhunen, J. (2000). Effects of long-term rainfall variability on evapotranspiration and soil water distribution in the Chihuahuan desert: A modeling analysis. Plant Ecology, 150, 145–159.
Sanborn, P., Bulmer, C., & Coopersmith, D. (2004). Use of wood waste in rehabilitation of landings constructed on fine-textured soil, central interior British Columbia, Canada. Western Journal of Applied Forestry, 19(3), 175–183.
Scherbina, V. V., Maltseva, I. A., & Solonenko, A. N. (2014). Peculiarities of postpyrogene development of algae in steppe biocenoses at Askania Nova Biospheric National Park. Contemporary Problems of Ecology, 7(2), 187–191.
Schneider, C. A., Rasband, W. S., & Eliceiri, K. W. (2012). NIH image to ImageJ: 25 years of image analysis. Nature Methods, 9(7), 671–675.
Seginer, I. (1969). The effect of albedo on the evapotranspiration rate. Agricultural Meteorology, 6(1), 5–31.
Sharma, M. L. (1985). Estimating evapotranspiration. Advances in Irrigation, 3, 213–281.
Shcherbyna, V. V., Maltseva, I. A., & Maltsev, Y. I. (2017). Post-pyrogenic changes in vegetation cover and biological soil crust in steppe ecosystems. Regulatory Mechanisms in Biosystems, 8(4), 633–638.
Shrestha, R. K., & Lal, R. (2008). Land use impacts on physical properties of 28 years old reclaimed mine soils in Ohio. Plant Soil, 306, 249–260.
Shrestha, R. K., & Lal, R. (2011). Changes in physical and chemical properties of soil after surface mining and reclamation. Geoderma, 161, 168–176.
Singh, P., Ram, S., & Ghosh, A. K. (2015). Changes in physical properties of mine soils brought about by planting trees. Ecology, Environment and Conservation Paper, 21, AS187–AS193.
Slabbers, P. J. (1980). Practical prediction of actual evapotranspiration. Irrigation Science, 1(3), 185–196.

Tasumi, M., & Allen, R. G. (2007). Satellite-based ET mapping to assess variation in ET with timing of crop development. Agricultural Water Management, 88(1), 54–62.
Teixeira, J. L., & Pereira, L. S. (1992). ISAREG, an irrigation scheduling model. ICID Bulletin, 41(2), 29–48.
Toy, T. J. (1979). Potential evapotranspiration and surfacemine rehabilitation in the Powder River Basin, Wyoming and Montana. Journal of Range Management, 32(4), 312–317.
Tromp-van Meerveld, H. J., & McDonnell, J. J. (2006). On the interrelations between topography, soil depth, soil moisture, transpiration rates and species distribution at the hill slope scale. Advances in Water Resources, 29, 293–310.
Williams, C. A., & Albertson, J. D. (2004). Soil moisture controls on canopy-scale water and carbon fluxes in an African savanna. Water Resources Research, 40(9), W09302.
Zeng, N., & Yoon, J. (2009). Expansion of the world's deserts due tovegetation-albedo feedback under global warming. Geophysical Research Letters, 36, L17401.
Zhukov, A. V., Andrusevich, K. V., Lapko, K. V., & Sirotina, V. O. (2015). Geostatistical estimation of soil aggregate structure as a composite variable. Biological Bulletin, 3, 101–121.
Zhukov, O. V., Kunah, O. N., & Novikova, V. A. (2016). The functional organisation of the mesopedobionts community of sod pinewood soils on arena of the river Dnepr. Visnyk of Dnipropetrovsk University, Biology, Ecology, 24(1), 26–39.